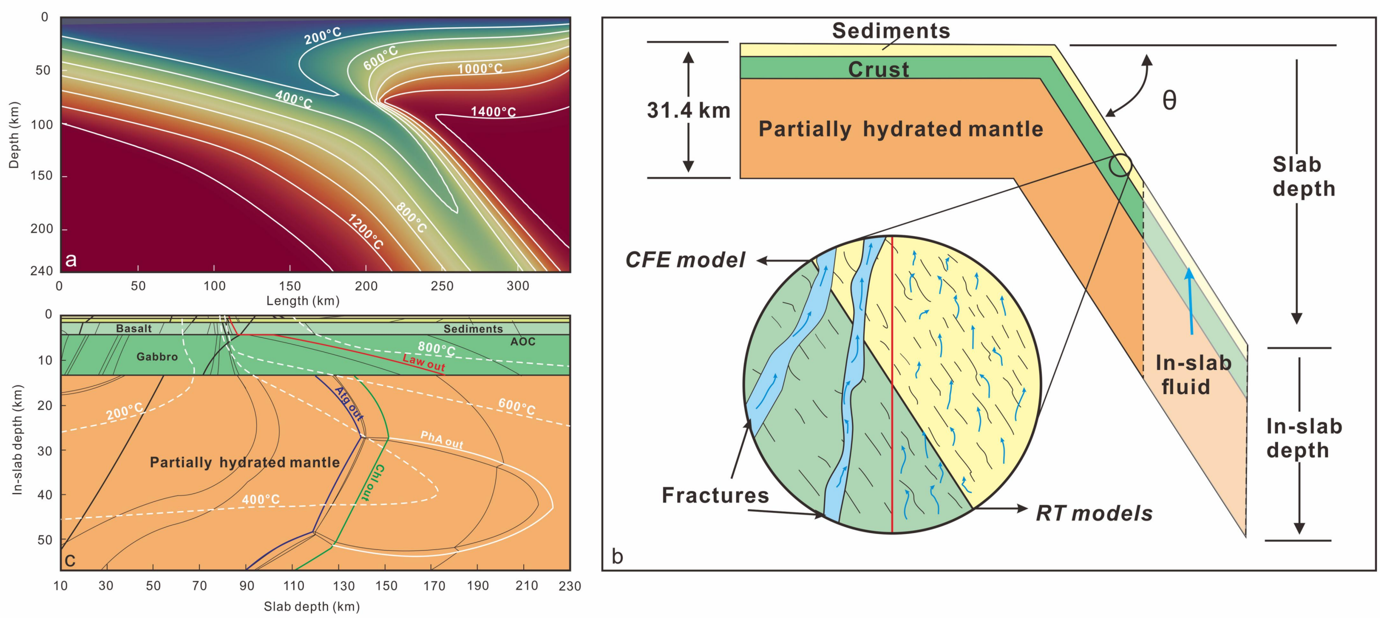

Fig. S1 (a) Temperature field of the plotted Mariana subduction profile using thermalmechanical modeling; (b) subduction slab devolatilization model configuration; the whole-rock composition is shown in Table S1; the lightly shaded trapezoidal region corresponds to the rectangular coordinate frame of Fig. S1c; (c) phase diagram of the Mariana subduction slab as a function of depth to the top of the slab and depth within the slab, see Figs. S1a and S1b for model geometry and conditions, particularly highlighting the hydrated minerals which influence the release of redox flux (lawsonite, antigorite, A-phase, and chlorite).

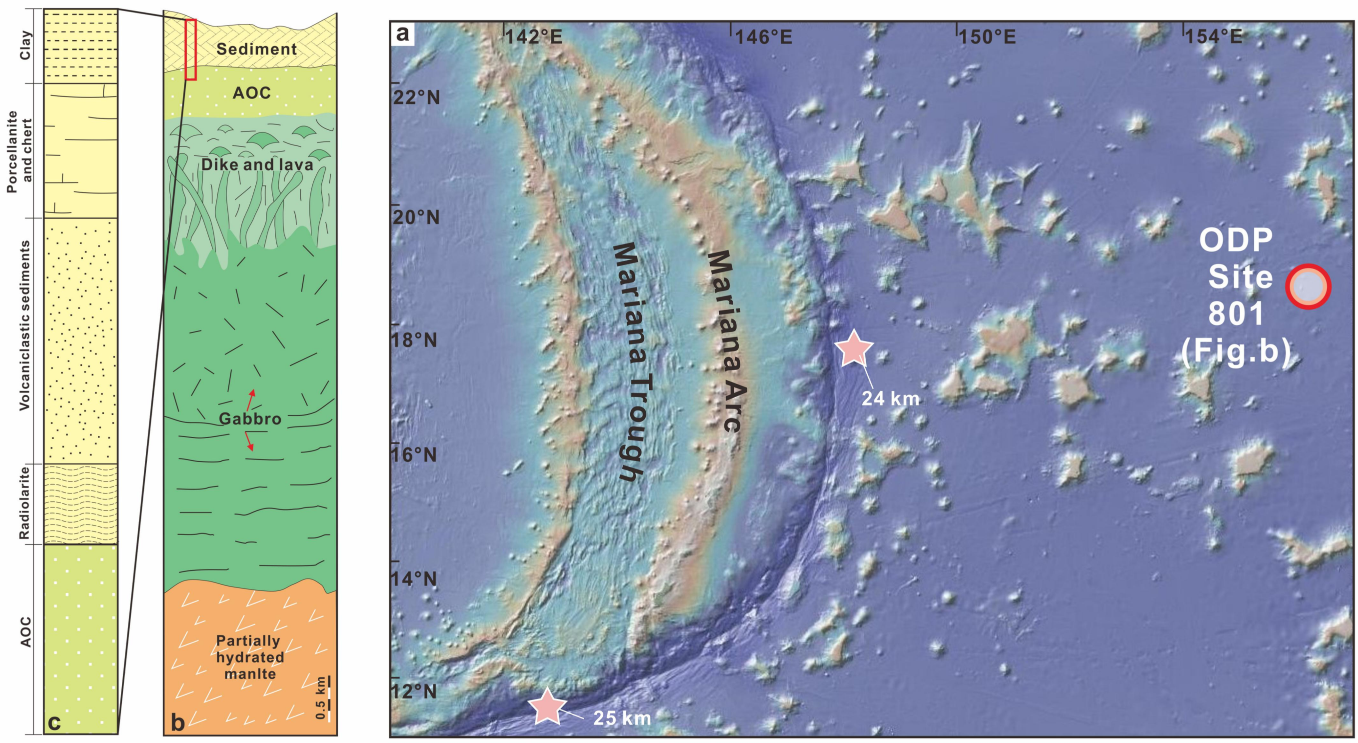

Fig. S2 (a) Location map for samples used in this study; the pink stars represent the thickness of the hydrated mantle at the location[24, 56]; (b-c) the rock types of the Mariana oceanic slab profile, and the corresponding thickness[8].

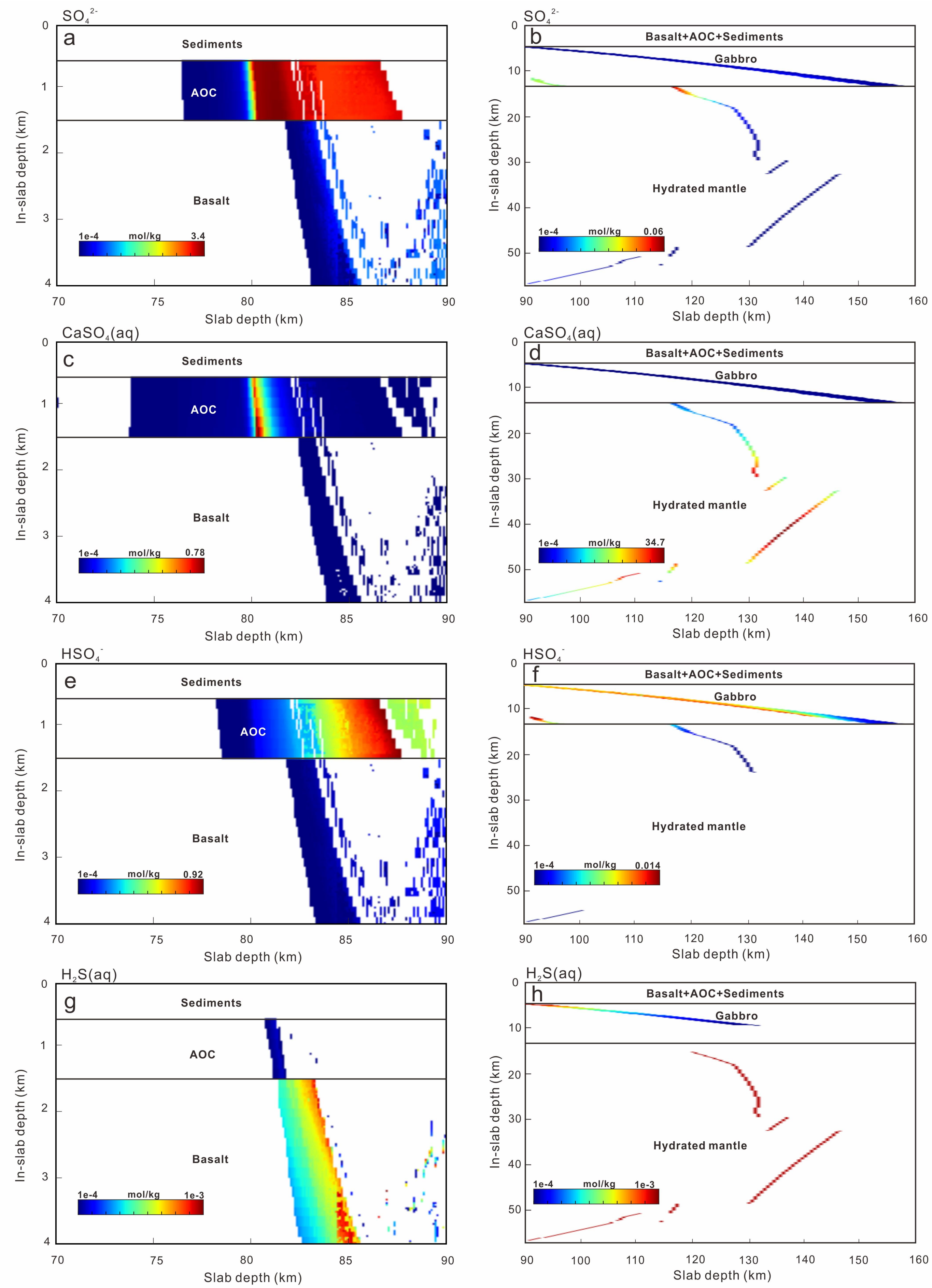

Fig. S3 The main sulfur oxidized species and reduced species and their concentrations in the fluid.

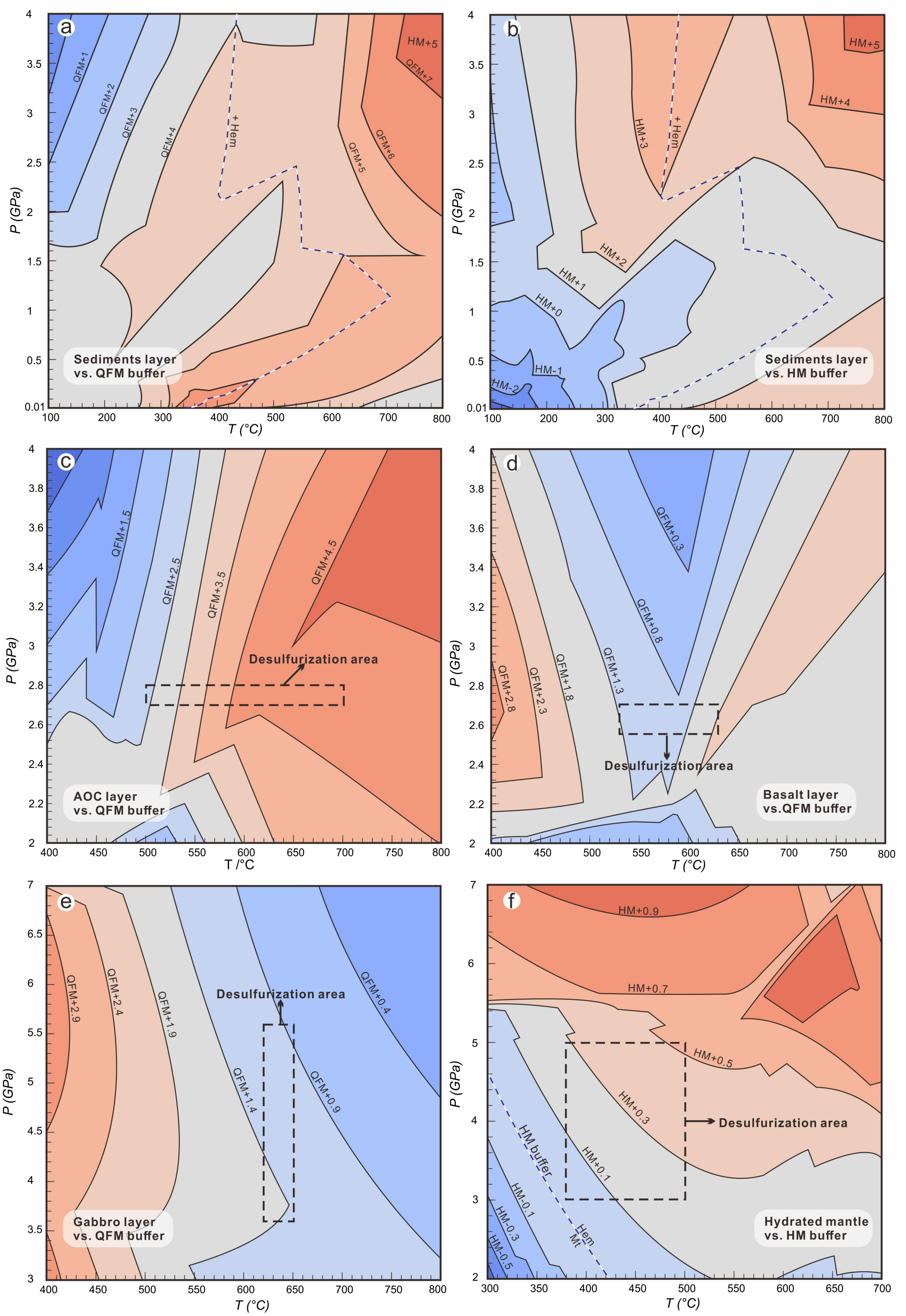

Fig. S4 The trend of oxygen fugacity in different rock layers varies with P-T conditions, and the black dashed box represents the corresponding oxygen fugacity during fluid release. QFM (quartz-fayalite-magnetite; in magnetite stability fields) or HM (hematite-magnetite; in hematite stability fields) buffers are used as evaluation criteria of the redox degree.

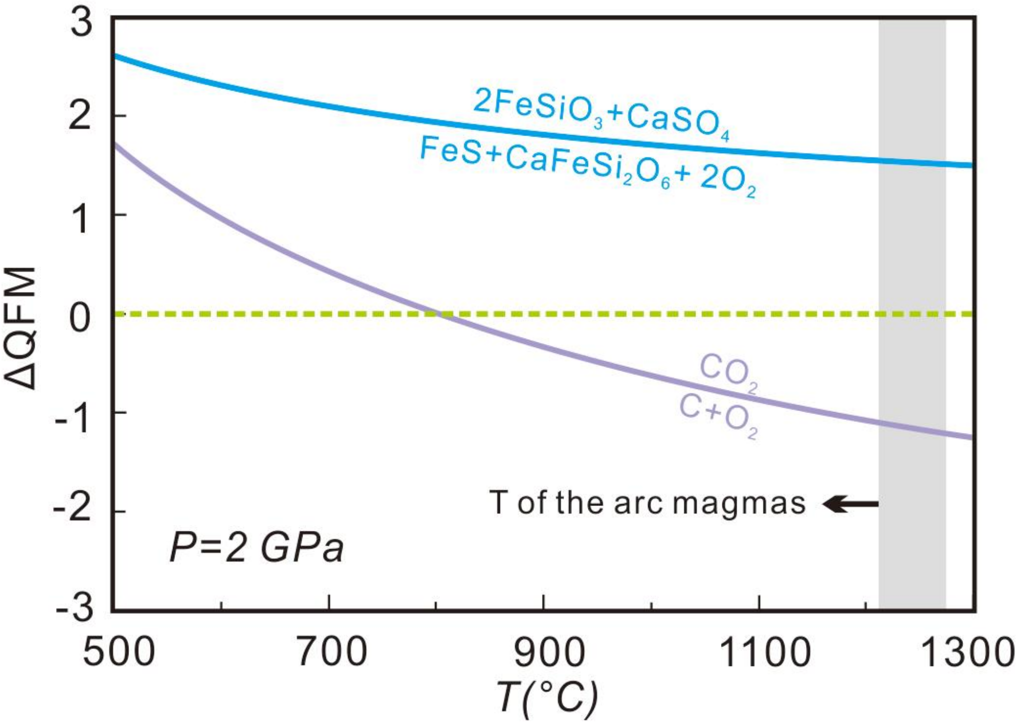

Fig. S5 The C + O_2 = CO_2 (CCO) and FeS + $CaFeSi_2O_6$ + $2O_2$ = $2FeSiO_3$ + $CaSO_4$ (SSO) buffer reactions as a function of temperature and oxygen fugacity at 2.0 GPa, modified from ref[12]; the dark area represents the temperature during the arc magma formation with the water content of 2-6 wt%[37].

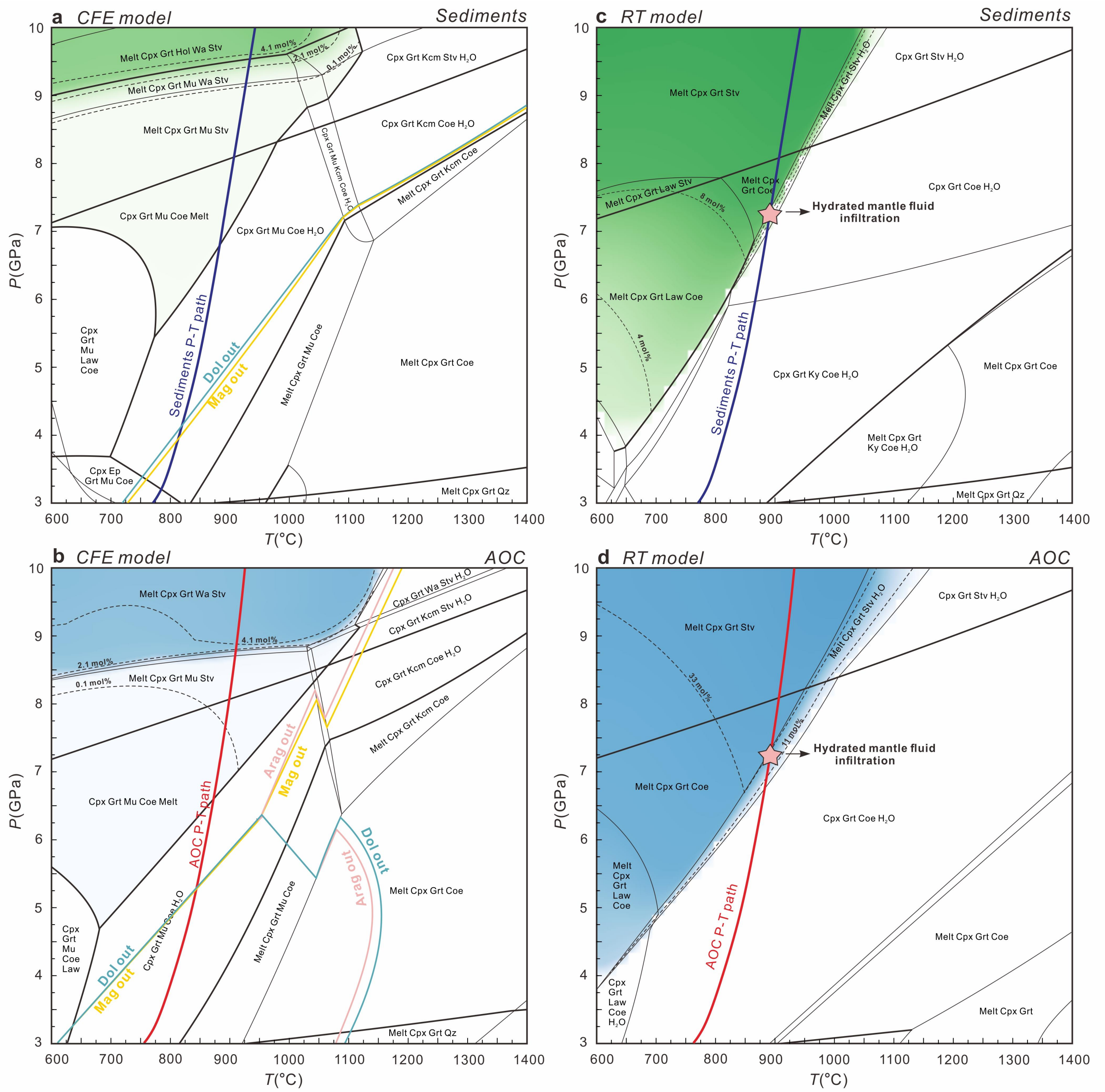

Fig. S6 P-T phase relationships of sediment and AOC; (a-b) P-T pseudosections show the partial melting at P = 8.7-9.7 GPa triggered by dehydration of white mica in the SDD model; (c-d) P-T pseudosections show the partial melting at P = ~7.3 GPa triggered by infiltration of fluids from the hydrated mantle in the FI model; the deepening shades of green and blue indicate an increase in melt contents.

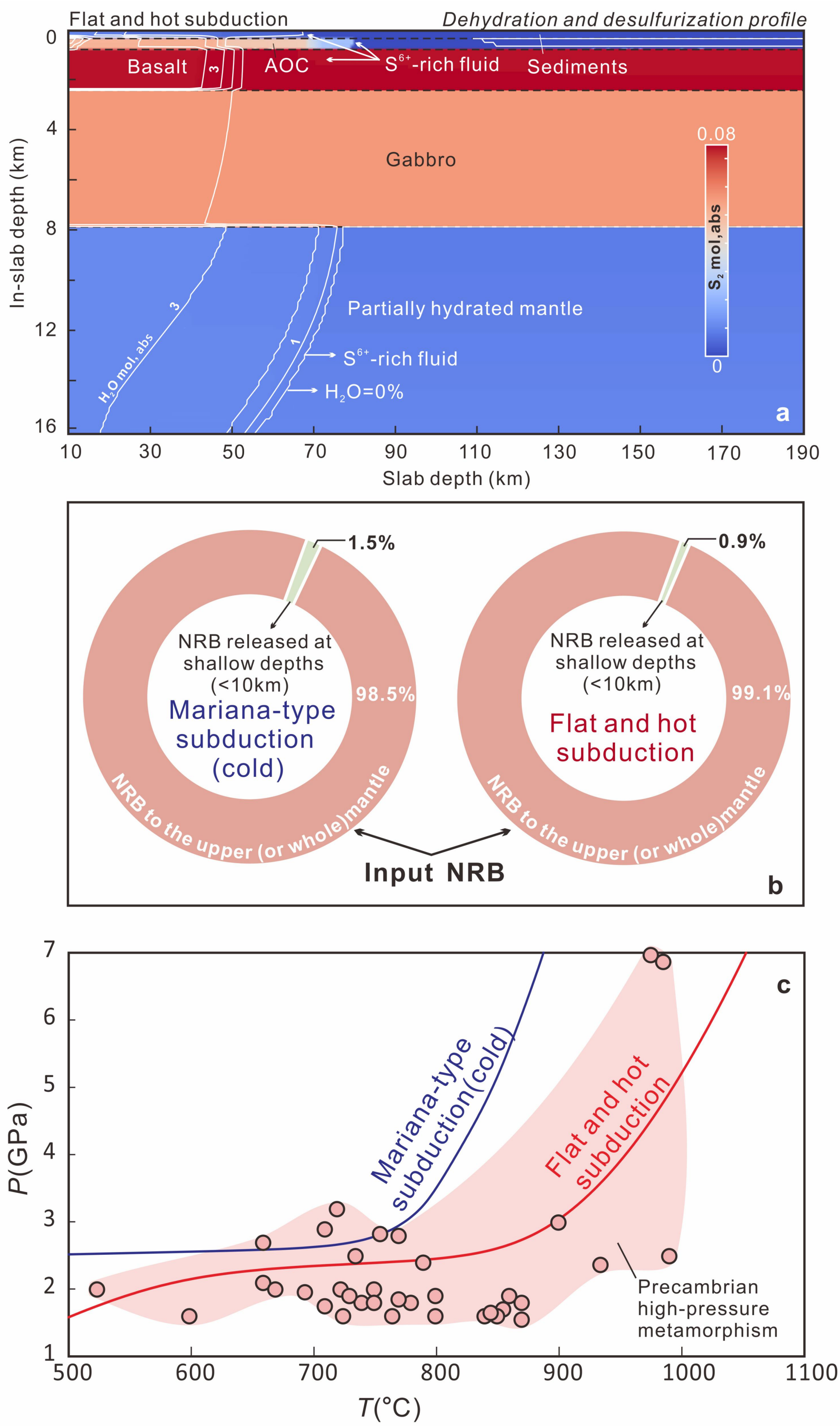

Fig. S7 (a) the 2D dehydration-desulfurization profile of the subduction slab in an flat and hot subduction case (Cascadia subduction), where the sulfur in the fluid is also mainly oxidized S^{6+} species; compared with Mariana-type subduction, hot subduction fluid release depth is shallower and oxidation flux into sub-arc mantle is less but is still enough to oxidize arc magma; the oxidation flux mainly comes from hydrated mantle (20% of S_{tot}), AOC (100% of S_{tot}), and sediments (40% of S_{tot}); (b) the mass balance calculation of oxidation flux contributed to the mantle in the Mariana-type subduction and Andean-type subduction indicates that the impact of subduction thermal structure on the oxidation of the upper or entire mantle is negligible; the average thickness of the hydrated mantle in this semi-quantitative calculation of the oxidation rate of upper mantle and whole mantle is estimated to be 7.8 km containing 2 wt% H_2O based on global observations; (c) comparison of P-T trajectories using hot and flat subduction with precambrian metamorphism (>1.5 Gpa; Brown and Johnson 2019) and Mariana-type subduction trajectories.

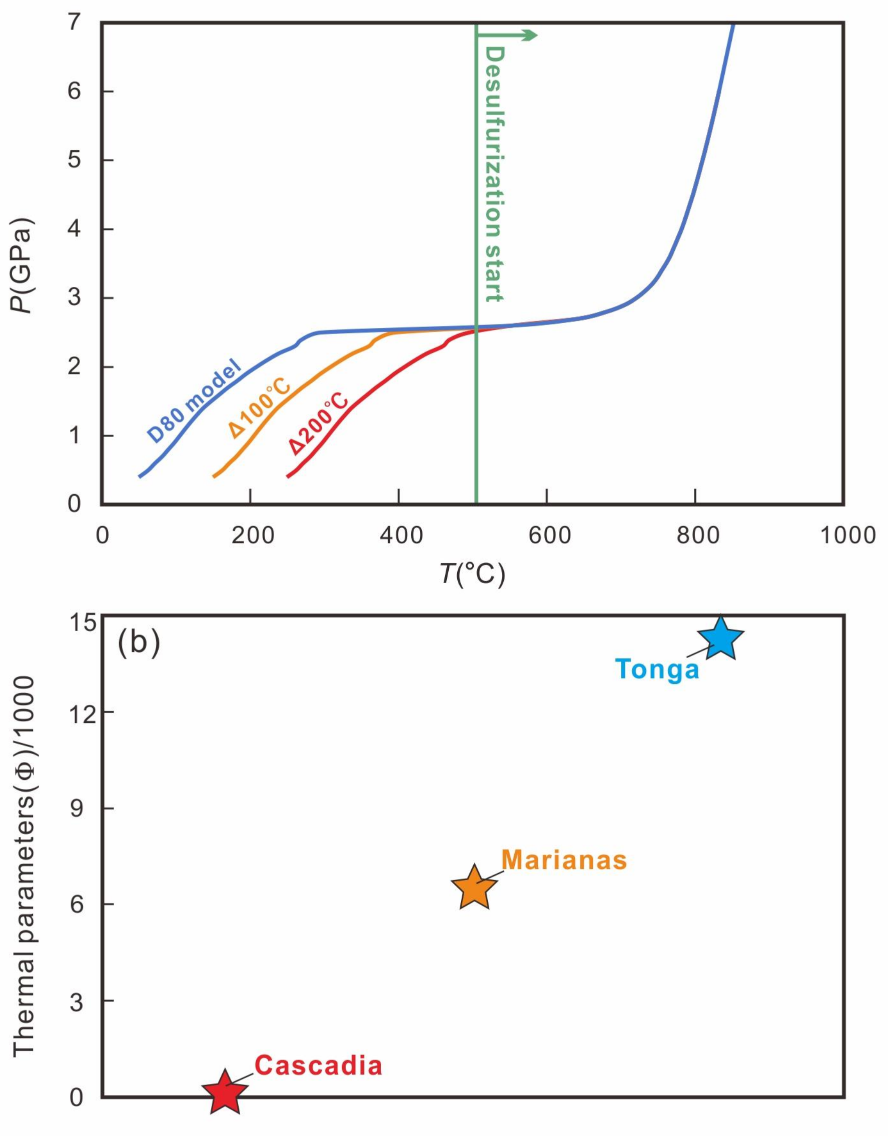

Fig. S8 (a) P-T paths of upper mafic and sediment layers; an increase of 200 °C at fore-arc depths (<2.5 GPa) represents the record of exhumed rocks[73]; these temperature increases did not affect the desulfurization; (b) Comparison of Mariana subduction with Cascadia (hot) and Tonga (very cold) subduction on thermal structures using subduction thermal parameters[50-51] as proxies.

Reference

Brown, M. & Johnson, T. Time's arrow, time's cycle: granulite metamorphism and geodynamics. Mineral. Mag. 83, 323-338 (2019).